Journal of Hydrology 557 (2018) 305–320

Contents lists available at ScienceDirect

Journal of Hydrology

journal homepage: www.elsevier.com/locate/jhydrol

Research papers

An integrated hydrological modeling approach for detection and attribution of climatic and human impacts on coastal water resources

Dapeng Feng [a], Yi Zheng [b,*], Yixin Mao [c], Aijing Zhang [a,d], Bin Wu [a], Jinguo Li [a], Yong Tian [b], Xin Wu [a]

[a] College of Engineering, Peking University, Beijing 100871, China
[b] School of Environmental Science and Engineering, Southern University of Science and Technology, Shenzhen 518055, Guangdong Province, China
[c] Civil and Environmental Engineering, University of Washington, Seattle 98195, WA, USA
[d] Bureau of South to North Water Transfer of Planning, Designing and Management, Ministry of Water Resources, Beijing 100038, China

ARTICLE INFO

Article history:
Received 7 November 2017
Received in revised form 13 December 2017
Accepted 14 December 2017
Available online 15 December 2017
This manuscript was handled by Corrado Corradini, Editor-in-Chief, with the assistance of Christophe Darnault, Associate Editor

Keywords:
Climate change
Human activities
Integrated surface water-groundwater modeling
Coastal area
Water resources
Groundwater

ABSTRACT

Water resources in coastal areas can be profoundly influenced by both climate change and human activities. These climatic and human impacts are usually intertwined and difficult to isolate. This study developed an integrated model-based approach for detection and attribution of climatic and human impacts and applied this approach to the Luanhe Plain, a typical coastal area in northern China. An integrated surface water-groundwater model was developed for the study area using GSFLOW (coupled groundwater and surface-water flow). Model calibration and validation were performed for background years between 1975 and 2000. The variation in water resources between the 1980s and 1990s was then quantitatively attributed to climate variability, groundwater pumping and changes in upstream inflow. Climate scenarios for future years (2075–2100) were also developed by downscaling the projections in CMIP5. Potential water resource responses to climate change, as well as their uncertainty, were then investigated through integrated modeling. The study results demonstrated the feasibility and value of the integrated modeling-based analysis for water resource management in areas with complex surface water-groundwater interaction. Specific findings for the Luanhe Plain included the following: (1) During the historical period, upstream inflow had the most significant impact on river outflow to the sea, followed by climate variability, whereas groundwater pumping was the least influential. (2) The increase in groundwater pumping had a dominant influence on the decline in groundwater change, followed by climate variability. (3) Synergetic and counteractive effects among different impacting factors, while identified, were not significant, which implied that the interaction among different factors was not very strong in this case. (4) It is highly probable that future climate change will accelerate groundwater depletion in the study area, implying that strict regulations for groundwater pumping are imperative for adaptation.
© 2017 Elsevier B.V. All rights reserved.

1. Introduction

The majority of the world's population, as well as some of the largest cities, are distributed along coastal areas. Access to sufficient clean water is vital to the socio-economic development of these areas. Coastal water resources have recently garnered significant research attention (Benini et al., 2016; Brinson et al., 2013; Chen et al., 2016; Sreeja et al., 2016; Zhang et al., 2015). Previous studies have shown that the hydrological processes in coastal areas could be profoundly influenced by climate change (Miller et al., 2003; Schnorbus et al., 2014; Stefanova et al., 2015) and intensive human activities (Teatini et al., 2006; White and Greer, 2006; Wu and Chen, 2013), such as water conservancy projects, agricultural irrigation, and urban water use. In many cases, the impacts of climate change and human activities are interconnected (Benini et al., 2016; Huang et al., 2013; Zhang et al., 2015) and are therefore difficult to assess.

Some studies have attempted to attribute the variation in water resources to the individual influences of climatic and human factors. A traditional approach evaluates paired catchments (Lørup et al., 1998; Zhao et al., 2010), but this application is limited due to difficulty in finding suitable paired catchments, especially at medium and large scales; this research approach is also expensive. A more popular approach is to perform a detrending analysis. In this approach, the impact of climate variability is identified and separated using statistical analyses (e.g., non-parametric tests, time series analysis, regression analysis, etc.), a hydrological sensitivity analysis, the elasticity method, a water balance calculation or

* Corresponding author.
E-mail address: zhengy@sustc.edu.cn (Y. Zheng).

https://doi.org/10.1016/j.jhydrol.2017.12.041
0022-1694/© 2017 Elsevier B.V. All rights reserved.

hydrological modeling; then, the remaining impacts can be attributed to human activities (Wang et al., 2013). However, the detrending approach usually lacks underlying physical mechanisms and assumes that the impacts of climate and human factors are independent, which may not be valid in many cases (Zhao et al., 2016). The third approach directly separates the impacts through physically based hydrological modeling. For example, Li et al. (2009) built a Soil and Water Assessment Tool (SWAT) model for an agricultural catchment on the Loess Plateau of China and simulated different climate and land use scenarios. The individual impacts of climate variability and land use change were then assessed through a series of scenario comparisons based on the modeling results. This modeling-based approach can address the interaction between these two factors but has rarely been applied to integrated surface water-groundwater modeling.

In water-limited areas where groundwater accounts for a large portion of the local water supply (Gorelick and Zheng, 2015; Wada et al., 2010), substantial and complex surface water (SW)-groundwater (GW) interactions would further complicate the interpretation of the individual and combined impacts of climate and human activities on coastal water resources. As mentioned before, most relevant studies have focused on surface water systems (Bao et al., 2012; Huang et al., 2013; Zhang et al., 2015). With regard to groundwater systems, many studies have addressed the individual impact of either climate (Ali et al., 2012; Green et al., 2011; Klove et al., 2014) or human activities (Cao et al., 2013; Liu et al., 2001; Pokhrel et al., 2015), but only a few studies attempted to quantify their collective impact (Li et al., 2014b; Pulido-Velazquez et al., 2015). Studies of integrated surface water-groundwater (SW-GW) systems are even rarer. Zhao et al. (2016) investigated the impact of climate variability and land use change on green and blue water resources in the Weihe River Basin of China using SWAT (Arnold et al., 2012), where the groundwater system was highly simplified. Landes et al. (2014) used MODFLOW (Harbaug, 2005), a groundwater flow model, to evaluate the influences of groundwater exploitation and climate change on wetland extensions. Groundwater recharge by infiltration was determined by an external water balance calculation. While the modeling-based approach is promising, the SW-GW interaction was highly simplified in these studies. Therefore, a fully integrated modeling approach is desired.

In recent years, some fully integrated SW-GW models have been developed and applied in different watersheds; these models include MIKE-SHE (Graham and Butts, 2005), HydroGeoSphere (Brunner and Simmons, 2012; Therrien et al., 2010), ParFlow (VanderKwaak and Loague, 2001), PAWS (Shen and Phanikumar, 2010), CATHY (Camporese et al., 2010), and GSFLOW (Markstrom et al., 2008). These dynamic and spatially distributed models usually simulate a 3-D groundwater system and a 1-D or 2-D surface water system. They can depict an integrated water resources system in great spatial and temporal detail and have been used to address a variety of water resource issues (Ajami et al., 2014; Goderniaux et al., 2009; Krause et al., 2007; Pérez et al., 2011; Tian et al., 2015). However, these complex models usually involve substantial simulation uncertainty (Wu et al., 2014), especially when the data for initialization, parameterization and calibration of the model are insufficient, therefore hindering the wider application of these models. Few studies have applied these models to investigate the climate and human impacts on an entire SW-GW system at a large basin scale.

This study performed integrated SW-GW modeling for the Luanhe Plain, a typical coastal area in northern China. This area is part of the downstream sector in the Luanhe River Basin (LRB) and is located in the northeastern North China Plain (Fig. 1). The LRB is one of the most sensitive areas to climate change in China (Jiang et al., 2015; Wang et al., 2015), and intensive human activities (e.g., large water transfer projects, and agricultural irrigation) have significantly altered the hydrological processes in this basin (Bao et al., 2012; Yan et al., 2012). The LRB has many water-related problems such as climate variability (Jiang et al., 2015), anthropogenic influences (Li et al., 2015; Wang et al., 2013), ecological deterioration (Yan et al., 2012), and drought (Li et al., 2014a). Previous hydrological modeling efforts (Jiang et al., 2015; Li et al., 2015; Yan et al., 2015) in the LRB have focused on its upper mountainous area, where surface runoff was the main concern. The complicated SW-GW interactions and responses to both climate change and human activities have not been systematically studied.

The main objectives of this study were as follows: (1) to demonstrate the feasibility and value of conducting an integrated SW-GW model for studying coastal water resources under significant data scarcity, (2) to couple integrated SW-GW modeling with modeling-based attributions for climatic and human impacts on water resources, and (3) to investigate how the water resources in the Luanhe Plain would respond to future climate change and evaluate the climate-induced risk of groundwater depletion in this area.

2. Data and methods

2.1. Study area

The Luanhe River Basin (LRB) is located in the northeastern North China Plain (NCP) (Fig. 1). It consists of two distinctive parts: the upper mountainous area and the lower plain area, the Luanhe Plain (Wang et al., 2015). The main Luanhe River, as well as several small coastal streams, drains water into the Bohai Sea. This study, which is concentrated on the Luanhe Plain, has a total area of approximately 7770 km^2. It is within the administrative boundaries of the cities of Tangshan and Qinghuangdao and covers eight counties, including Fengnan, Tanghai, Luanxian, Luannan, Leting, Lulong, Changli, and Funing. The first five counties are in the western and southern parts of the plain and are governed by Tangshan, and the remaining three are in the northeastern part of the plain and are governed by Qinhuangdao. This coastal plain typically has a temperate continental climate. The annual mean temperature is approximately 10–11 °C, the annual precipitation is approximately 620 mm, and the annual actual evapotranspiration (ET) accounts for approximately 90% of the precipitation. The precipitation has significant seasonal variation and mostly occurs in July and August. The study area has relatively flat topography, and the elevation ranges from 0 m on the south shore area to 68 m in the north. The dominant land use type on the plain is farmland, which accounted for approximately 62% of the total area as of 2010. Approximately 55% of the farmlands have substantial irrigation. The main crops in the study area are grain crops, including winter wheat, summer maize and rice. Some high-value crops, such as cotton and peanuts, are also planted in this region but account for no more than 20% of the farmlands (or no more than 12% of the total area).

A major surface water diversion, the Yanshan headwork, was built approximately 1 km downstream from the Luanxian gauging station (see Fig. 1). The headwork is a major point from which a substantial portion of the Luanhe River flow is diverted to irrigate the farmlands on the plain. Groundwater is also a major water source for regional irrigation. Since the 1970s, groundwater exploitation in this area has increased rapidly, mainly due to growing irrigation needs and municipal water demands. Furthermore, several large reservoirs and inter-basin water transfer projects have been built in the upper LRB, including the Panjiakou, Daheiting, and Taolinkou reservoirs and two well-known transfer projects. One delivers water from the Luanhe River to Tianjin, and

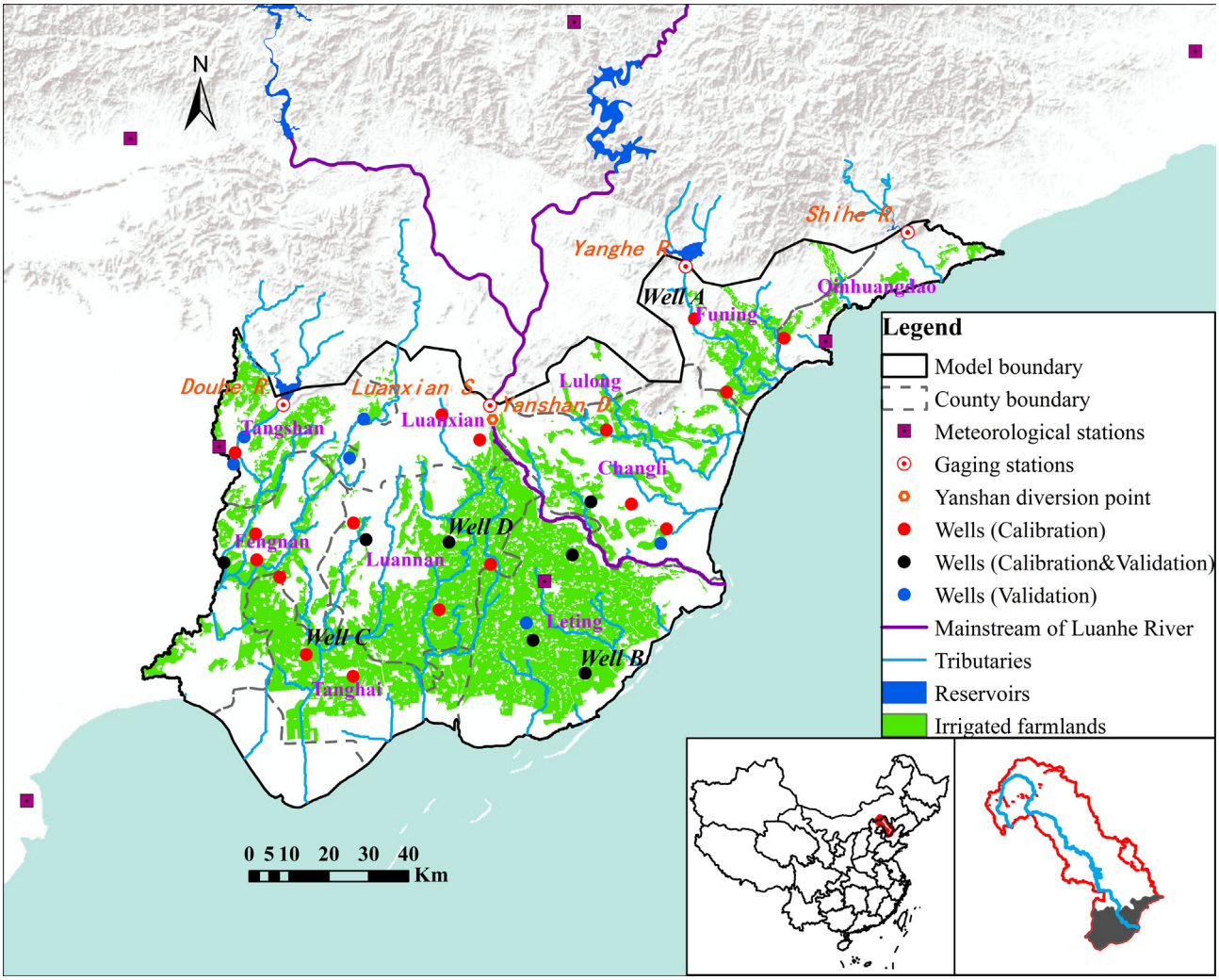

Fig. 1. The study area and modeling domain.

the other delivers water to Tangshan; these two water transfer projects were established in 1983 and 1985, respectively (Wang et al., 2015). The reservoirs and water transfer projects profoundly influenced streamflow from the mountainous area to the plain.

2.2. The GSFLOW model

This study developed an integrated surface water-groundwater (SW-GW) model for the Luanhe Plain using GSFLOW (coupled groundwater and surface-water flow). GSFLOW (Markstrom et al., 2008) is an integrated modeling tool developed by the U.S. Geological Survey (USGS) that has been successfully applied in many different hydrological contexts (Carroll et al., 2017; Doherty and Hunt, 2009; Hassan et al., 2014; Huntington and Niswonger, 2012; Surfleet and Tullos, 2013; Tian et al., 2015). The GSFLOW model reproduces all the major processes of the terrestrial water cycle. It is comprised of three modules; a surface module for simulating surface water and root zone soil water, a subsurface module for modeling vadose zone flow and groundwater flow, and a stream-lake module that routes water through surface water bodies. The surface module uses the PRMS (precipitation-runoff modeling system) (Leavesley et al., 1983), and the subsurface and stream-lake modules use MODFLOW (Harbaug, 2005), a classic groundwater flow model. In the GSFLOW model, the 2-D surface domain is delineated into hydrologic response units (HRUs) in terms of either irregular polygons or regular grids. The subsurface domain is separated vertically into multiple layers based on hydrogeological information and horizontally delineated into finite difference grids. A simulation of SW-GW exchange is a critical part of modeling. GSFLOW introduces the concept of a gravity reservoir that enables water exchange between a surface HRU and its linked subsurface grid(s). However, direct exchange between an aquifer cell and its connected river or lake segment(s) is calculated based on Darcy's law. More details about the USGS version of GSFLOW can be found elsewhere (Markstrom et al., 2008).

A digital elevation model (DEM), land cover map and soil type map are the basic geographic data used to parameterize a GSFLOW model. For the Luanhe Plain, a DEM with 90-m resolution was acquired from the Shuttle Radar Topography Mission (SRTM, USA) and used to determine the highest elevations based on MODFLOW grids and streambeds. A digitized land cover map (1:100,000) in 1980 and soil type map (1:1,000,000) were acquired from the Heihe Program Data Management Centre (www.heihedata.org) and were the basis for the initial parameterization of the HRUs. Horizontally, the modeling domain was delineated into 7770 regular grids (1 km × 1 km) for both the surface and subsurface. The subsurface modeling domain was vertically separated into three layers: one shallow aquifer layer and two deep aquifer layers, which was based on previous groundwater modeling studies for the entire North China Plain (Cao et al., 2013; Liu et al., 2011,

2008). Details on how the layers were conceptualized based on available hydrogeological data can be found in previous studies. The stream network was divided into 194 segments, and any portion of the river segment that intersected a MODFLOW grid was referred to as a "reach." There are 2016 reaches total in this model.

Meteorological data and boundary inflow data were the key inputs used to drive the model simulations. In this study, daily meteorological data, primarily daily temperatures (maximum and minimum) and precipitation, were collected at seven meteorological stations within or adjacent to the study area (Fig. 1). The point observations were then interpolated to each HRU using the square inverse distance weighting method. Because it is a coastal plain without significant topographical changes, the uncertainty associated with the data interpolation based on seven stations would be relatively small, especially for temperature. On the other hand, this study focused on the long-term water budget of the entire area rather than the spatiotemporal distributions of hydrological variables within the area. According to the interpolated data, the annual average precipitation of the study area was 615 mm, which was very close to the estimate from local meteorological agencies (approximately 620 mm). Uncertainty in the spatial distribution of precipitation and its impacts on the simulated long-term water budget are further investigated in Section 2.4.

Daily streamflow rates at four boundary-gauging stations (Fig. 1) were used as the surface boundary inflow conditions. For groundwater modeling, the northern plain received subsurface lateral flow from the mountainous area and was represented using a specified groundwater inflow boundary condition. However, the flux of the subsurface lateral flow was largely unknown. According to reports by the Haihe River Commission (Haihe River Chronicle Compilation Committee et al., 1994), the annual flux of the groundwater inflow was possibly between 0.1 and 0.5 billion m^3. The annual flux was adjusted within this range during model calibration (see Section 2.3). Furthermore, the coastline in the south was set to a specified groundwater head boundary condition of zero (i.e., sea level), and the west boundary was set to no-flow conditions due to the existence of a groundwater divide.

The agriculture in the Luanhe Plain used surface water and groundwater conjunctively. The water management practices, including surface water diversion, groundwater pumping and irrigation, have significantly changed the natural water cycle and need to be properly reflected in the model. As GSFLOW does not simulate agricultural irrigation based on environmental parameters (e.g., temperature and soil moisture), agricultural water use data must be prepared externally. In this study, annual water diversion volumes at the Yanshan diversion point were determined based on the literature (Haihe River Chronicle Compilation Committee et al., 1994; Wang and Liu, 2010). The annual diversion varied between 0.55 and 1.38 billion m^3 from 1977 to 2000. In the model, the diverted water was evenly distributed on all farmland HRUs. Monthly variations in diversion volume were based on the crop growth cycle, and the same was assumed for all farmland HRUs. Each month, the daily diversion was assumed to be constant. Annual pumping rates in different stress periods were determined based on references (Haihe River Chronicle Compilation Committee et al., 1994; Huang and Lin, 1991; Zhao, 2009). Unfortunately, spatially and temporally detailed pumping data were not available, which is a common challenge for basin-scale groundwater modeling. To derive daily time step simulations within each stress period, constant daily pumping rates were assumed for the growing season, and zero pumping was assumed for non-growing season. Spatially, the total volume of groundwater was first allocated to different counties in proportion to their crop yields. Then, within each county, the allocated volume was evenly distributed to all the HRUs of irrigated farmland. The groundwater was applied to where it was pumped.

The above spatial and temporal treatment of the pumping data inevitably involved significant uncertainty. Nevertheless, they represented our best estimation given data scarcity. Because this research focused on assessing and separating basin-scale hydrological responses to climate change and human activities, the spatial and temporal uncertainties may not significantly affect the major conclusions of this study and will be later investigated (see Section 2.4 for the approach).

2.3. Model calibration and validation

The entire calibration procedure was finished manually. The groundwater model parameters (i.e., hydraulic conductivities and specific yields) were adopted from previous modeling studies of the North China Plain, which includes the Luanhe Plain (Cao et al., 2013; Liu et al., 2011, 2008). Details on how the parameter values were determined can be found in the references. Note that the computational grid in previous studies was 2 km × 2 km, which has been refined to 1 km × 1 km in this study. As a regular step in running MODFLOW, a steady-state simulation was first performed to set the initial conditions for the subsequent transient simulation. In this step, the subsurface lateral inflow was manually adjusted between 0.1 and 0.5 billion m^3/a and was eventually set to 0.286 billion m^3/a, where the steady-state simulation can appropriately reproduce the observed groundwater levels since 1975. After the steady-state simulation, a transient simulation was performed for the period between 1975 and 2000. The first two years (i.e., 1975–1976) were treated as a "spin-up" period to produce reasonable initial soil water conditions for subsequent years (Tian et al., 2015), and they were excluded from the following analyses. The subsequent years were further divided into four stress periods: 1977–1980, 1981–1990, 1991–1993, and 1994–2000. Monthly groundwater level data from 24 monitoring wells (see Fig. 1) during 1977–1983 were collected from local government agencies for the model calibration. As some data were missing, approximately 1500 data points were eventually used for calibration. In the calibration stage, to better match the simulated water levels with the observed ones, the initial pumping rates were moderately adjusted. If the model significantly and consistently underestimated or overestimated the observed water levels in the specific area and stress period, the initial county-wide pumping rate associated with the area and stress period was tuned within a range of ±10%, while keeping the total pumping rate of the entire Luanhe Plain approximately unchanged for that stress period. In some local areas, groundwater model parameters were also tuned to further improve the water level simulation. The above steps represent a common calibration procedure in groundwater modeling. It is worth emphasizing that, with limited water level observations, there would be no unique calibration for a complex groundwater model. To examine the adequateness of the calibration, the model validation was performed for the fourth stress period (1994–2000) using data from a previous study (Liu et al., 2011).

Unfortunately, no streamflow observations were available to calibrate the PRMS model (i.e., the surface hydrology module in GSFLOW) because there were no official gauging stations within the study area except for the four boundary sites (see Fig. 1). Alternatively, the average runoff coefficients and annual ET rates (without human interference) in this area, as reported by local hydrological handbooks, were referenced. By adjusting key PRMS parameters (e.g., maximum possible area contributing to surface runoff, soil maximum available capillary water-holding capacity and maximum depth where evapotranspiration can occur), the model was run with all irrigation, pumping and division practices turned off (i.e., a scenario with no human interference), and the simulated long-term runoff coefficients and evapotranspiration were calculated and compared against values reported in the refer-

ences. It is worth noting that such a data scarcity situation actually reflects the strength of integrated surface water-groundwater modeling, rather than a shortcoming of this study. In a recent study (Yao et al., 2017), MODFLOW with its Streamflow Routing package (SFR2) was applied to quantify the mountain block recharge in the Qinghai-Tibet Plateau in a situation that had no groundwater level observations and only streamflow observations could be referred.

2.4. Analysis of input uncertainty

Due to the data limitation, the uncertainty of key model inputs, including the subsurface lateral inflow, precipitation, and pumping rates, was significant. To examine the impact of input uncertainty on the modeling results, four modeling experiments were conducted (see Table 4). Compared to the original modeling (i.e., the calibrated model), each experiment had one change in model inputs. In Experiment 1 and Experiment 2, the annual groundwater inflow equaled 0.1 and 0.5 billion m^3, respectively. These two volumes defined the range within which the groundwater inflow was adjusted in the steady-state simulation. In Experiment 3, for each simulation time step, all the HRUs were assigned the basin-wide average precipitation. Experiment 3 was for examining whether the spatial distribution of precipitation would have a notable impact on the modeling results. In Experiment 4, instead of using a constant annual pumping rate for each stress period, we assumed that the rate was linearly increasing, while keeping the multiyear average rate fixed. This experiment was utilized for investigating whether the coarse temporal resolution of pumping data would significantly affect the modeling results. The simulation results of the four experiments were compared against those of the original model for the period from 1977 to 2000. Note that all four hypothetical experiments represented extreme situations. Thus, the comparison results indicated the upper limits of modeling uncertainty, rather than the actual modeling uncertainty.

2.5. The attribution approach

This study investigated how different natural and human-related forces would individually and collectively impact water resources in the Luanhe Basin. The 1990 s (i.e., 1991–2000) and 1980 s (i.e., 1981–1990) were chosen as the two decades for comparison. Mann-Kendall (M−K) tests were conducted to detect any significant trends in key forces during the entire simulation period (1975–2000). Because the presence of autocorrelation can affect trend detection (Hamed and Rao, 1998; Yue et al., 2002), an autocorrelation analysis was conducted prior to a trend test. If a lag-1 autocorrelation was identified, the method of Yue et al. (2002) was employed to pre-whiten the time series. In higher-order autocorrelation situations, the M-K test followed the method from Hamed and Rao (1998). Nonparametric rank sum tests were also performed to check any statistically significant differences between the two decades. Five variables were considered on an annual time scale to represent key natural and human driving forces, including maximum temperature (T_{max}), minimum temperature (T_{min}), precipitation, total upstream inflow and total surface water diversion. Spatial average values were considered for the first three meteorological variables. The test results are presented in Table 1. As the statistics indicate, temperature had a strong increasing tendency from the 1980s to the 1990s. For precipitation and upstream inflow, although the test results were not significant, the differences between the two decades are notable regarding the ten-year average values, as indicated by the last column in Table 1. For surface water diversion, however, all statistics indicated no significant difference between the 1980s and 1990s. Groundwater pumping and land use change were also important human-related forces that impacted water resources. The pumping magnitude in this area has increased rapidly since the 1970s due to intensified human activities (Zhao, 2009). On the other hand, by comparing digitized land use maps from 1980 and 1995, the change in irrigated farmland area during 15 years was only 1.4%.

Based on the above analysis, T_{max}, T_{min}, precipitation, upstream inflow and groundwater pumping were identified as the key variables needed to develop scenarios for comparison. The first three meteorological variables represent climate conditions within the Luanhe Plain (hereafter referred to as the climate factor), the upstream inflow reflected the combined impact of climate conditions and human activities in the upstream area (hereafter referred to as the upstream factor), and groundwater pumping represented the impact of human activities (hereafter referred to as the human factor). The climate and human factors were key model inputs which drove the GSFLOW simulations, while the upstream factor was the surface boundary condition of the model. Five scenarios (see Table 2) were then developed, representing different combinations of the three factors. A ten-year GSFLOW simulation was performed for each scenario. To guarantee the same initial conditions, all five ten-year simulations were started after the same transient simulation from 1977 to 1990. Scenario O is the baseline scenario that represents the actual conditions in the 1990s (i.e., 1991–2000). Scenario D represents the actual conditions in the 1980s (i.e., 1981–1990). Scenarios A, B and C all have one factor that is different from Scenario O. Therefore, by comparing Scenarios A, B and C against Scenario O, the individual impacts of climate variability, change in upstream inflow, and change in groundwater withdrawal could be assessed, respectively. A comparison between Scenario D and Scenario O revealed the combined effect of all three factors. The following equations were used to separate the individual effects of the climate factor (P_c), upstream factor (P_u), and human factor (P_h), as well as the synergy or counteraction between them (P_s).

$$P_c = \frac{\Delta I_c}{\Delta I} \times 100\% \quad (1)$$

$$P_u = \frac{\Delta I_u}{\Delta I} \times 100\% \quad (2)$$

$$P_h = \frac{\Delta I_h}{\Delta I} \times 100\% \quad (3)$$

$$P_s = \frac{\Delta I - \Delta I_c - \Delta I_h - \Delta I_u}{\Delta I} \times 100\% \quad (4)$$

Here, ΔI_c, ΔI_u, and ΔI_h represent the changes caused by the individual climate factor, upstream factor and human factor, respectively, and ΔI stands for the overall difference between the 1980s and 1990s. It holds that $P_c + P_u + P_h + P_s = 1$, and P_s can be either positive or negative. The model output variables considered in the attribution analysis included river outflow, groundwater level, ET and water volume of net SW-GW exchange. All these output variables were calculated as annual average.

2.6. Future climate scenarios

A simple sensitivity analysis was first conducted to examine how water resources in the Luanhe Plain would respond to climate change. Temperature changes of 0 °C, 1 °C, 2 °C, 3 °C, and 4 °C, and precipitation changes of 0%, ±5%, ±10%, and ±15% were assumed, which lead to 35 combinations of temperature and precipitation changes, each representing a future hypothetical climate scenario. In all these scenarios, the surface water diversion, groundwater pumping and agricultural irrigation were kept at historical levels. Comparison of the scenarios would reveal the sensitivity of the

Table 1
Statistical analyses on temporal trends for five key variables.

Variable	M-K test			Rank-sum test		Mean difference [4]
	Z[1]	Significance level [2]	Slope (β) [3]	Rank-sum	Significance level [2]	–
T_{max}	3.678	$p < 0.01$	0.0401 °C/a	82	$p < 0.1$	0.57 °C
T_{min}	7.577	$p < 0.01$	0.0685 °C/a	64	$p < 0.01$	0.94 °C
Precipitation	−1.367	ns	−5.30 mm/a	125	ns	−88 mm (−13.5%)
Diversion	1.626	ns	0.0055 billion m^3/a	93	ns	0.010 billion m^3/a (1.1%)
Upstream inflow	−0.868	ns	−0.067 billion m^3/a	95	ns	0.97 billion m^3/a (54.9%)

[1] Z is the test statistic of the M-K test (Hirsch et al., 1982; Yue et al., 2002). A positive (negative) value of Z indicates a potential upward (downward) trend in the time series.
[2] "ns" indicates that the trend or difference was not significant at the 0.90 significance level (i.e., p greater than 0.1).
[3] The slope was calculated using the Theil-Sen's slope estimator (Sen, 1968; Theil, 1950).
[4] The difference was calculated as the average value of the 1990s minus that of the 1980s. The values in parentheses indicate the relative changes from the 1980s to 1990s.

Table 2
Scenarios developed for assessing individual and combined impacts.

Scenario	Climate factor	Upstream factor	Human factor
O	1990s	1990s	1990s
A	1980s	1990s	1990s
B	1990s	1980s	1990s
C	1990s	1990s	1980s
D	1980s	1980s	1980s

water resources to climate change. Such an analysis is common in water resource impact assessments.

A more systematic assessment was also performed by using outputs from selected Earth System Models (ESMs). Table 3 lists the 21 ESMs considered in the assessment. Previous studies demonstrated that these models have an adequate performance in the North China Plain (NCP), where the study area is located (Chen et al., 2013; Chen et al., 2014; Du et al., 2014; Fu et al., 2009; Ouyang et al., 2016; Wang et al., 2015; Xing et al., 2014). The ESM data were obtained from phase 5 of the Coupled Model Intercomparison Project (CMIP5) model archive (http://cmip-pcmdi.llnl.gov/cmip5/) for the medium stabilization scenario (i.e., RCP4.5) and the high radiative forcing scenario (i.e., RCP8.5) (van Vuuren et al., 2011). The change factor (CF) method (Wilby and Harris, 2006) was deployed to downscale outputs of the ESMs, which is a widely used and robust method for impact analyses of non-extreme variables (Chen et al., 2011; Diaz-Nieto and Wilby, 2005; Jackson et al., 2011; Morrison et al., 2002; Ouyang et al., 2015). Change factors were first derived by calculating the differences between background years (1975–2000) and future years (2075–2100) based on the ESMs. Then, historical weather observations during 1975–2000 were perturbed by the change factors to establish respective climate scenarios for the years 2075–2100. The GSFLOW model was run with 42 total climate scenarios (i.e., the 21 ESMs under the two emission scenarios), with surface water diversion, groundwater pumping and agricultural irrigation kept at historical levels. The modeling results were then used to assess the water resources under climatic uncertainty.

Note that keeping diversion, groundwater and irrigation at historical levels did not imply that the agricultural water use is irresponsive to climate change. It actually reflects the strict water resources regulation currently enforced in China. The central government has set a "redline" for water resource exploitation at the national scale, and local governments and river basin authorities

Table 3
Descriptions of the ESMs from CMIP5 applied in this study.

ID	Model	Institution	Country
1	BNU-ESM	Beijing Normal University	China
2	CCSM4	National Centre for Atmospheric Research (NCAR)	United States
3	CMCC-CMS	Centro Euro-Mediterraneo per i Cambiamenti Climatici	Italy
4	CNRM-CM5	Centre National de Recherches Météorologiques / Centre Européen de Recherche et Formation Avancée en Calcul Scientifique	France
5	CSIRO-Mk3.6.0	Commonwealth Scientific and Industrial Research Organization in collaboration with Queensland Climate Change Centre of Excellence	Australia
6	CanESM2	Canadian Centre for Climate Modelling and Analysis	Canada
7	FGOALS-g2	LASG, Institute of Atmospheric Physics, Chinese Academy of Sciences and CESS, Tsinghua University	China
8	FIO-ESM	The First Institute of Oceanography, SOA, China	China
9	GFDL-CM3	NOAA Geophysical Fluid Dynamics Laboratory	United States
10	GFDL-ESM2M	NOAA Geophysical Fluid Dynamics Laboratory	United States
11	GISS-E2-H	NASA Goddard Institute for Space Studies	United States
12	GISS-E2-R	NASA Goddard Institute for Space Studies	United States
13	HadGEM2-AO	National Institute of Meteorological Research/Korea Meteorological Administration	South Korea
14	IPSL-CM5A-MR	Institut Pierre-Simon Laplace	France
15	MIROC-ESM	Japan Agency for Marine-Earth Science and Technology, Atmosphere and Ocean Research Institute (The University of Tokyo), and National Institute for Environmental Studies	Japan
16	MIROC5	Atmosphere and Ocean Research Institute (The University of Tokyo), National Institute for Environmental Studies, and Japan Agency for Marine-Earth Science and Technology	Japan
17	MPI-ESM-MR	Max-Planck-Institut für Meteorologie (Max Planck Institute for Meteorology)	Germany
18	MRI-CGCM3	Meteorological Research Institute	Japan
19	NorESM1-M	Norwegian Climate Centre	Norway
20	BCC-CSM1.1	Beijing Climate Centre, China Meteorological Administration	China
21	INM-CM4	Institute for Numerical Mathematics	Russia

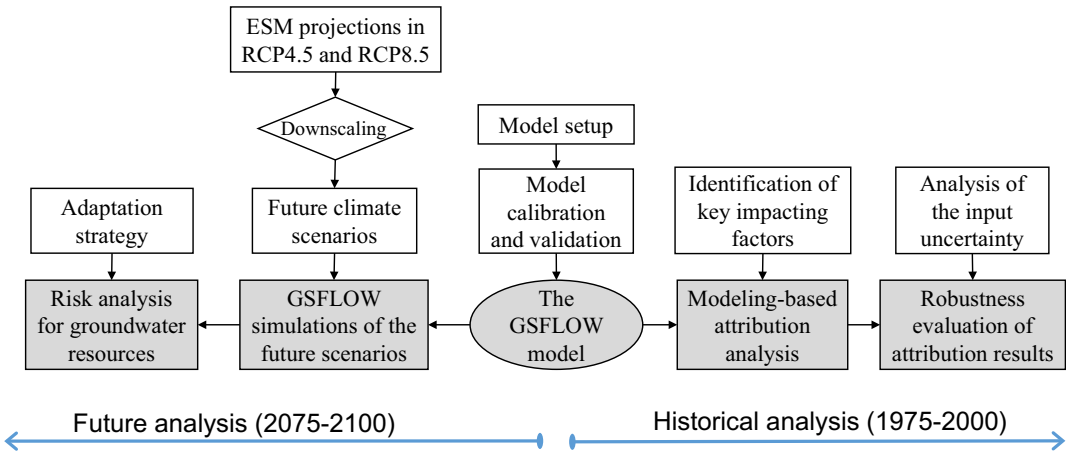

Fig. 2. The models and analyses performed in this study.

all have their own "redlines". In the NCP, where water resources are in a serious shortage, the agricultural water use was unlikely to increase in the future due to the "redline" regulation. Thus, the change in agricultural water use for the Luanhe Plain is largely policy-driven, rather than climate-driven. Furthermore, to mitigate the rapid drawdown of the groundwater table in the NCP, the local governments are making all possible efforts to reduce pumping. To reflect the water policy, the GSFLOW model was also run for the 42 future climate scenarios (2075–2100) at three reduced levels of pumping: 75%, 50% and 25% of historical levels.

The flow chart in Fig. 2 summarizes the modeling and analyses performed in this study.

3. Results and discussion

3.1. Calibration and validation results

As mentioned before, we had no observed streamflow data for a formal goodness-of-fit analysis. Alternatively, we adjusted the key parameters of the PRMS module to ensure an adequate model representation of the region's water budget. After the parameter adjustments, the simulated long-term average runoff coefficient for the study area was 0.15, and the simulated average annual ET was 563 mm, accounting for approximately 90% of the average annual precipitation. These simulation results were achieved with diversion, pumping and irrigation processes turned off and were consistent with values reported in the Hydrological Handbooks of Tangshan City and Qinhuangdao City (the Luanhe Plain is within these two cities' administrative boundaries) and other studies (Wang et al., 2002; Xia and Li, 2001). The reported values also represent the natural water cycle without human intervention.

Fig. 3a compares the simulated and observed average groundwater levels from 1977 to 1983. Each circle represents one of the 24 monitoring wells (see Fig. 1). All of the circles were very close to the 45-degree line, and only three had a deviation of over 2 m. The mean error, root mean square error, and coefficient of determination (R^2) were 0.059 m, 1.220 m and 0.984, respectively. The results indicated that, after the manual calibration, the model can adequately reproduce a spatial distribution of the groundwater level from a long-term average perspective. It is worth emphasizing that the calibration was not aimed at precisely reproducing the dynamics of the groundwater level at individual wells, as the dynamics could be notably disturbed by pumping practices common in this region; unfortunately, we had no temporally or spatially detailed information about these practices. Moreover, the groundwater level was measured at specific locations, but each MODFLOW grid represented a 1 km × 1 km area. Thus, given the scarcity of pumping data and the mismatch of spatial scales, it was not reasonable to expect that the model simulation results would nicely match the observed time series. Nevertheless, at some of the wells, the calibrated model still satisfactorily reproduced groundwater dynamics, such as at Well A, Well B and Well C in Fig. 1. The calibration results for these three wells are presented in Fig. 3b, c and d, respectively. The model performed especially well for Well A probably because it is very close to a tributary and, therefore, its change in water level was dominated by stream-groundwater interactions and was much less impacted by pumping practices. Some results of the model validation are presented in Fig. 4. Fig. 4a compares the simulated and observed average groundwater levels between 1994 and 2000 at the 13 monitoring wells (see Fig. 1). The mean error, root mean square error and R square were −0.45 m, 3.61 m and 0.94, respectively. The goodness-of-fit was acceptable, although not as good as in the calibration stage. Fig. 4b and 4c provide two examples of model validation at individual wells. Similarly, a perfect match was not expected in these cases.

Overall, as the above results indicate, after the manual calibration, the GSFLOW model can adequately reflect the long-term regional characteristics of the water cycle in the Luanhe Plain. Due to the lack of streamflow observations, however, the model simulation would have substantial uncertainty with regard to seasonal variability of streamflow. Thus, the impact analysis will focus on the annual amount of streamflow, rather than intra-annual characteristics of hydrographs such as flood peaks and low flow conditions.

3.2. Basin-wide water budget

Fig. 5 illustrates the average water budget from 1977 to 2000 based on the model simulation. Precipitation and ET were the largest inflow and outflow items, respectively, and upstream surface water (SW) inflow and outflow were the second largest items. Groundwater (GW) inflows and outflows were small. However, the SW-GW exchanges were much more substantial, and the groundwater pumping led to a notable groundwater storage decrease. Fig. 5 also shows that the agricultural irrigation significantly altered the basin-wide water cycle, particularly the SW-GW interaction. As the numbers in the parentheses indicate, if all of the pumping, diversion and irrigation practices were stopped, the SW-GW exchanges would have been dramatically altered, and there would have been approximately 17% less ET, 19% more

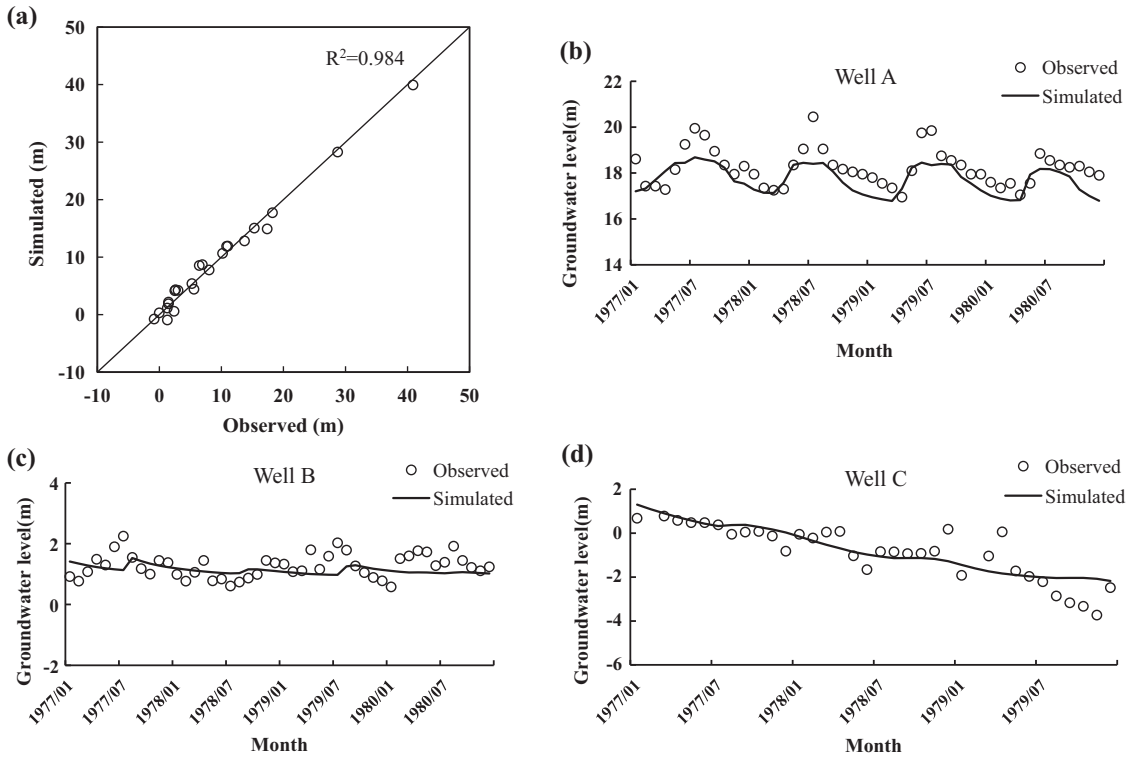

Fig. 3. The calibration results of groundwater level. (a) Average groundwater levels (1977–1983) at the 24 monitoring wells. Each well is represented by a circle; (b), (c) and (d) are monthly groundwater levels observed at wells A, B and C (see Fig. 1), respectively.

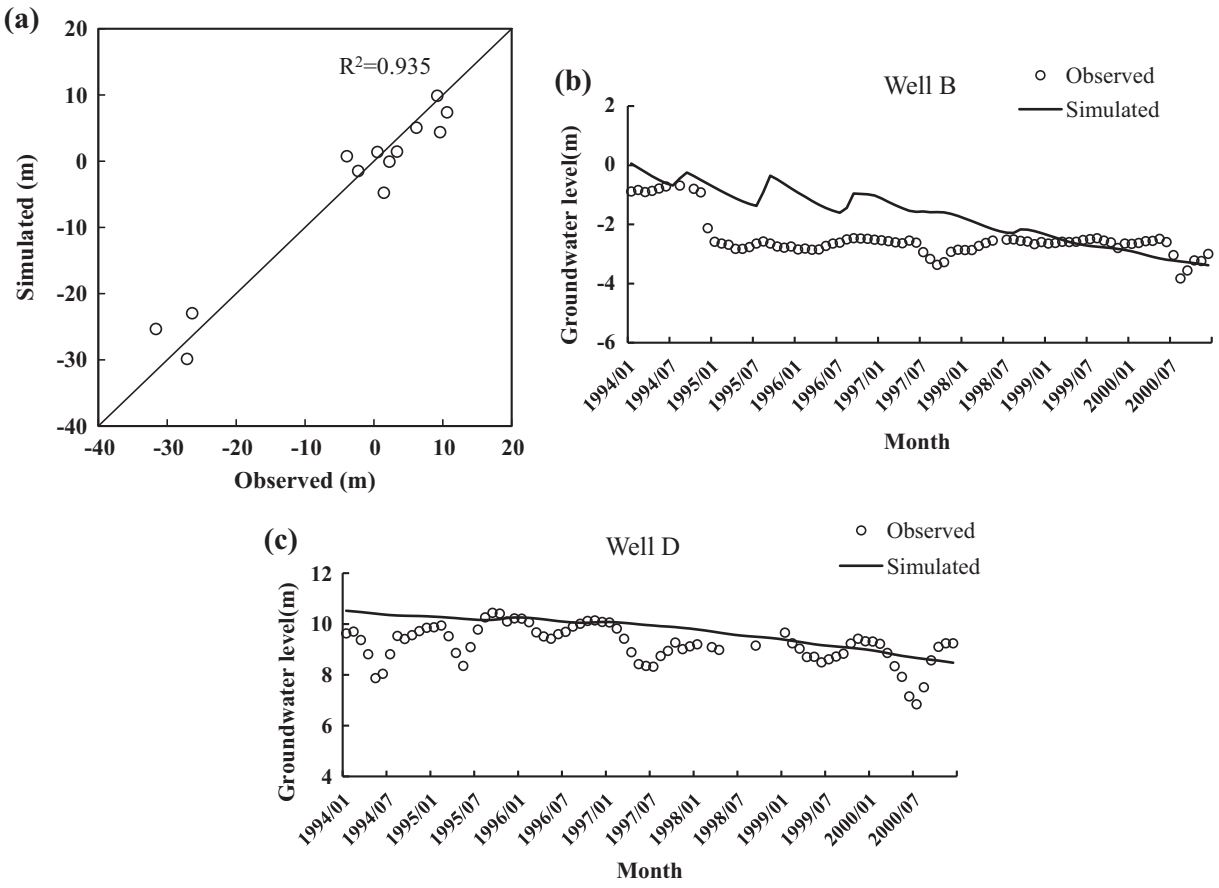

Fig. 4. The validation results for groundwater levels. (a) Average groundwater level (1994–2000) at the 13 monitoring wells; (b) and (c) show monthly groundwater levels observed at wells B and D (see Fig. 1), respectively.

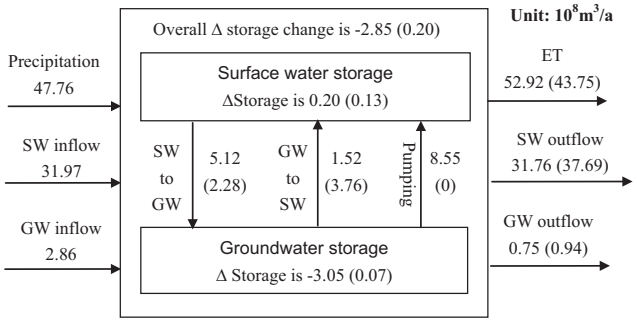

Fig. 5. The simulated water budget of the Luanhe Plain (1977 to 2000). The numbers in parentheses indicate the corresponding values if all pumping, diversion and irrigation practices were stopped.

outflow to the Bohai Sea, and relatively stable (even slightly increased) groundwater storage.

Fig. 6a shows the annual outflow to the Bohai Sea as simulated by the GSFLOW model. The three driving forces of local precipitation, inflow from the upstream mountainous area, and surface water division were plotted as well. The figure shows how the outflow has been largely controlled by upstream inflow. The difference between the inflow and the outflow was quite small during the simulation period and correlated with local precipitation. From 1979 to 1980, both the inflow and the outflow dropped dramatically because a large reservoir, the Panjiakou Reservoir, began storing water in December of 1979. The diversion was relatively stable, with an average value of 0.96 billion m^3/a, and its impact on the outflow was trivial. However, the regional groundwater level continued to decrease since the late 1970 s (see Fig. 6b) at a rate of approximately 0.4 m/a, which was largely due to increased pumping. The severe groundwater depletion may lead to various ecological and environmental problems, such as wetland degradation, seawater intrusion, and land subsidence (Cao et al., 2013; Landes et al., 2014; Werner et al., 2013), which have been observed in other parts of the North China Plain. In the next section, the impacts of different factors on regional water resources will be further explored.

Through the modeling experiments introduced in Section 2.4, we further investigated how input uncertainties would impact simulation of the basin-wide water budget. Table 4 summarizes the results for four key variables. For both ET and surface outflow (i.e., streamflow into the ocean), none of the four experiments demonstrated significant changes in the variables. On the other hand, in Experiment 3 and Experiment 4, all four variables were insensitive to input changes. This indicates that, with regard to

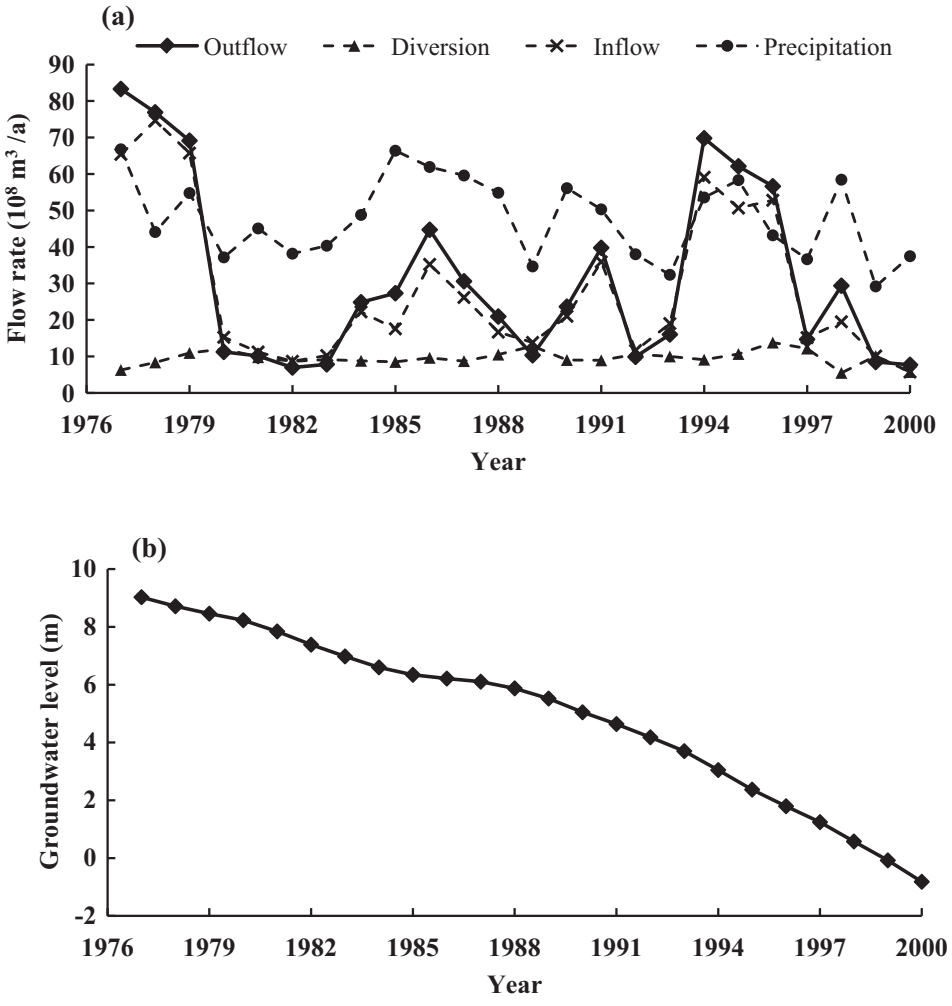

Fig. 6. Temporal change in key hydrological variables for the Luanhe Basin from 1977 to 2000. (a) Annual outflow, diversion, inflow and precipitation; and (b) The regional average groundwater level based on the model simulation.

Table 4
Results of the input uncertainty analysis.

Modeling Experiment	Change of model inputs	ET		Surface outflow		GW storage change		Net SW-GW exchange	
		Simulated (10^8 m^3/a)	δ [1] (%)	Simulated (10^8 m^3/a)	δ [1] (%)	Simulated (10^8 m^3/a)	δ [1] (%)	Simulated (10^8 m^3/a)	δ [1] (%)
Original	–	52.92		31.76		−3.05		3.60	
1	GW inflow 0.1 billion m^3/a	52.52	−0.8	31.34	−1.3	−3.54	16.0	4.30	19.5
2	GW inflow 0.5 billion m^3/a	53.41	0.9	32.71	3.0	−2.79	−8.5	2.21	−38.7
3	Homogeneous precipitation	53.05	0.2	31.64	−0.4	−3.04	−0.2	3.61	0.2
4	Linearly increasing pumping rate	52.85	−0.1	31.74	−0.1	−2.87	−6.1	3.78	4.9

[1] δ stands for the relative change between a hypothetical experiment and the original modeling. A negative (positive) value indicates that the input change would cause a decrease (increase) of the variable.

the basin-wide water budget, uncertainties associated with the spatial distribution of precipitation (Experiment 3) and temporal variability of pumping (Experiment 4) have very limited impacts on the simulation results. Significant differences in GW storage change and net SW-GW exchange are evident when the GW inflow is changed from 0.286 billion m^3/a (i.e., the calibrated value) to 0.1 billion m^3/a in Experiment 1 and 0.5 billion m^3/a in Experiment 2. It is worth re-emphasizing that all four experiments represented extreme situations, and the results in Table 4 indicate the upper limits of the modeling uncertainty, rather than the actual modeling uncertainty. In addition, whether the uncertainty of groundwater inflow would significantly affect the attribution analysis will be further addressed in Section 3.4.

3.3. Results of the attribution

GSFLOW simulations were performed for the five hypothetical scenarios in Table 2, and Table 5 summarizes the comparison results. Ten-year average values are presented for ET, surface outflow, net SW-GW exchange and groundwater level. The Δ values in the table reflect the individual and combined impacts of the three factors on different hydrological variables. The decomposed contribution percentages, calculated with Eqs. 1 through 4, are further illustrated in Fig. 7. As Fig. 7a demonstrates, the decrease in basin-wide ET was largely caused by the climate factor, and the effect of the human factor was not negligible but in the opposite direction. This decrease is not likely due to temperature change, as temperatures increased from the 1980 s to 1990 s, and the ET in this area was water-limited rather than energy-limited. The decrease must be attributed to the change in available water, which mainly consisted of local precipitation and agricultural irrigation. As Table 1 and Fig. 6a demonstrate, from the 1980 s to 1990 s, as local precipitation decreased, the diversion remained stable, and pumping increased. Thus, the decrease in ET (refer to Table 5) should be attributed to the decrease in local precipitation.

Fig. 7b shows that the upstream factor had the most significant impact on the change in river outflow to sea, followed by the climate factor (in the opposite direction); the human factor was the least influential. On the other hand, for both groundwater level (Fig. 7c) and net SW-GW exchange (Fig. 7d), the human factor dominated their changes, followed by the climate factor. Fourth, impacts from the three factors synergized with regard to ET, river outflow and net SW-GW exchange (Fig. 7a, b and d, respectively) but counteracted with regard to groundwater level (Fig. 7c). Nevertheless, the synergetic and counteractive effects were not significant in all four cases, which implies that the interaction among the three factors was not very strong with regard to the selected variables. The counteractive effect (Fig. 7c) can be explained as follows. In a warmer and drier climate, less infiltration led to a decrease in groundwater recharge, and lower instream flow led to an increase in groundwater discharge. These two effects collaboratively lowered the groundwater storage. However, pumping (i.e., the human factor) decreased groundwater heads, and higher surface inflow (i.e., the upstream factor) increased surface water heads. This would enhance groundwater recharge and reduce groundwater discharge and, therefore, mitigate the decline in groundwater storage caused by climate change.

Overall, the above decomposition analysis revealed that the impacts of different factors on the basin water cycle are complicated. The value of the integrated modeling approach used in this study was also well demonstrated.

3.4. Robustness of the attribution approach

As discussed in Section 3.2, the potential uncertainty of boundary groundwater inflow could lead to significant variability of groundwater storage changes and net SW-GW exchange. To investigate whether the attribution approach was robust under significant input uncertainty, the decomposition in Section 3.3 was repeated for both Experiment 1 and Experiment 2 (refer to Table 4). Fig. 8 compares the decomposition results from the original mod-

Table 5
Comparison of the five scenarios to identify the individual and collective impacts of the three factors.

Scenario	ET		Outflow		Groundwater level		Net SW−GW exchange	
	Simulated (10^8 m^3/a)	Δ [1] (10^8 m^3/a)	Simulated (10^8 m^3/a)	Δ [1] (10^8 m^3/a)	Simulated (m)	Δ [1] (m)	Simulated (10^8 m^3/a)	Δ [1] (10^8 m^3/a)
O	50.88		31.45		2.07		4.73	
A	55.34	−4.46	33.45	−2.00	2.21	−0.14	5.04	−0.31
B	51.16	−0.28	21.39	10.06	1.97	0.09	4.68	0.05
C	49.60	1.27	29.95	1.50	3.88	−1.81	3.43	1.30
D	54.53	−3.65	21.77	9.67	3.90	−1.84	3.65	1.08

[1] Δ stands for the difference between a scenario and the baseline scenario (i.e., Scenario O). A negative (positive) value indicates that the corresponding change(s) from the 1980 s to 1990 s would cause a decrease (increase) in the variable. The Δ values for Scenario A reflect the individual impact of the climate factor (i.e., ΔI_c in Eq. (1)); the Δ values of Scenario B reflect the individual impact of the upstream factor (i.e., ΔI_u in Eq. (2)); the Δ values of Scenario C reflect the individual impact of the human factor (i.e., ΔI_h in Eq. (2)); and the Δ values of Scenario D reflect the combined impact of all the three factors (i.e., ΔI).

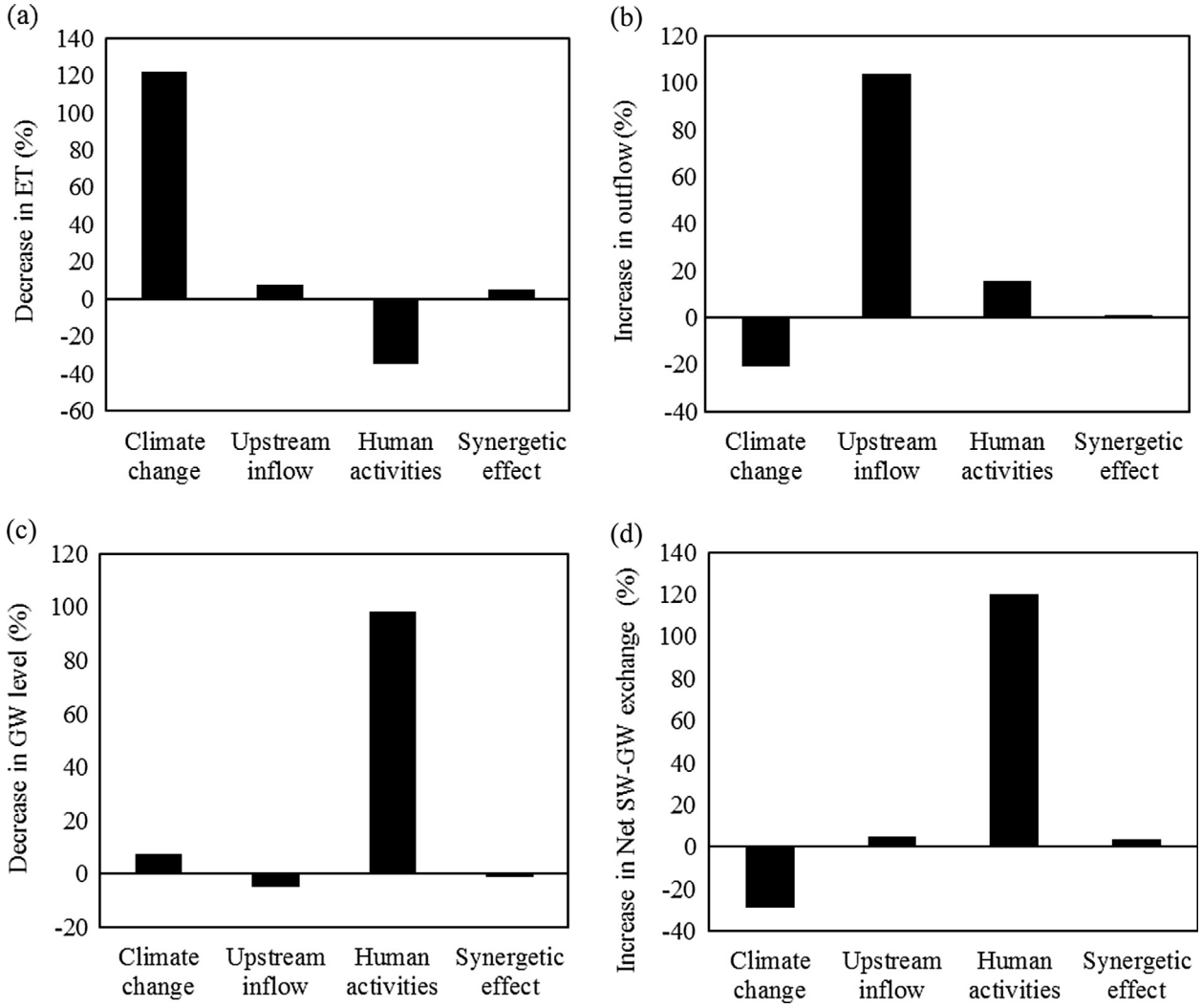

Fig. 7. Decomposition of the contribution of three impacting factors to the variation in key hydrological variables. (a) Change in evapotranspiration (ET); (b) change in river outflow; (c) change in groundwater level; and (d) change in net SW-GW exchange.

eling case with those in Experiment 1 and Experiment 2. The figure clearly demonstrates that the results in the three modeling cases are very similar, which proves the robustness of the attribution approach.

3.5. Sensitivity to climate change

As indicated by Fig. 7, in the study area, the climate factor contributed to approximately 21% of river outflow variability (as a measure of the surface water resource) and approximately 8% of groundwater level variability (as an indicator of the groundwater resource). Thus, regional water resource management must account for future climate change and be adaptive. Fig. 9 presents the results of the simple sensitivity analysis (see Section 2.6). First, higher temperatures led to smaller river outflow and faster groundwater declines, whereas higher precipitation increased river outflow and slowed down groundwater declines. Thus, increased precipitation could offset the negative impact of warming on the plain's water resources. Second, at a higher temperature level, a decline in both river outflow and groundwater were less sensitive to precipitation changes. This implies that, if the temperature keeps rising, the offsetting effect of precipitation would be reduced. Third, groundwater declines were more sensitive to the changes than river outflow, which means that the plain's groundwater resource is more vulnerable in a changing climate with regard to overall quantity. For example, assuming a 4 °C temperature increase occurring simultaneously with a 15% increase in precipitation, river outflow would increase by approximately 2% (Fig. 9a), while the GW decline would increase by approximately 4% (Fig. 9b). A more detailed analysis of the responses of water resources to potential climate change is provided in the next section.

3.6. Future risk of groundwater depletion

Fig. 10 shows the projected changes of annual mean temperature and precipitation under both RCP4.5 and RCP8.5. The 21 ESMs have different projections. However, all predicted an increase in temperature, and 19 out of 21 predicted an increase in precipitation. The ensemble averages for temperature increases were 2.6 °C and 4.9 °C under RCP4.5 and RCP8.5, respectively. The ensemble averages of the precipitation increase are 14.1% and 23.2% under RCP4.5 and RCP8.5, respectively. This warmer and wetter tendency was consistent with previous studies in this region (Fu et al., 2009; Li et al., 2015; Wang et al., 2015; Yuan et al., 2005). Fig. 11 illustrates how the seasonal variations in temperature and precipita-

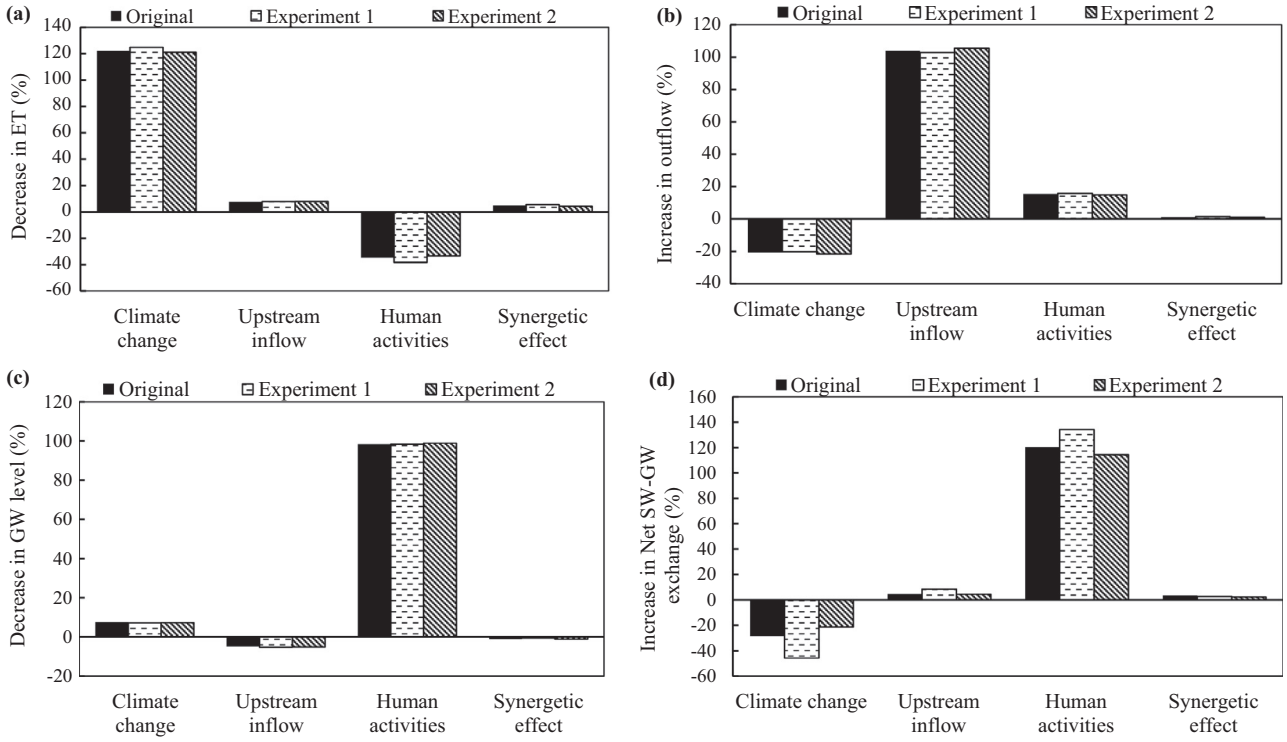

Fig. 8. Comparison of the decomposition results in the original modeling and the two hypothetical modeling experiments. (a) Change in evapotranspiration (ET); (b) change in river outflow; (c) change in groundwater level; and (d) change in net SW-GW exchange.

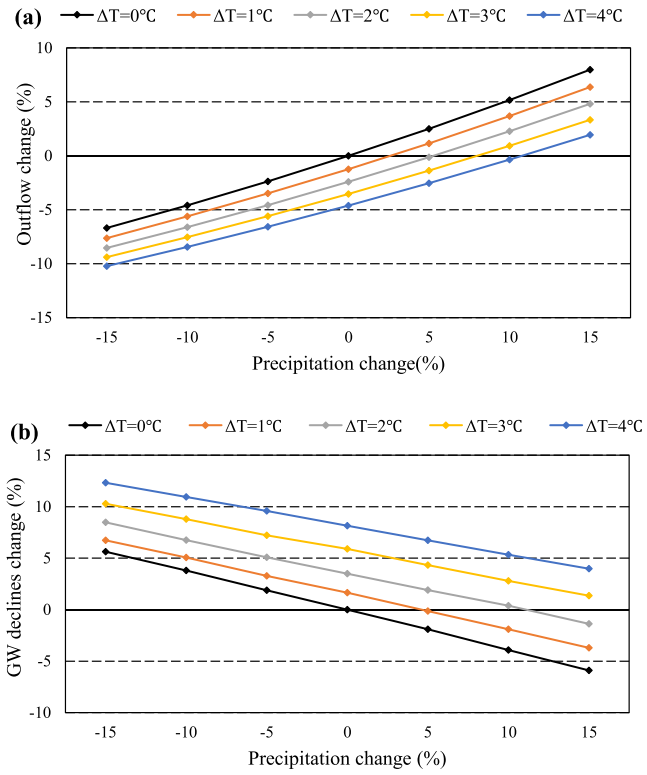

Fig. 9. Sensitivity of both surface water and groundwater resources to hypothesized climate changes. (a) Percentage change in river outflow and (b) percentage change in groundwater declines.

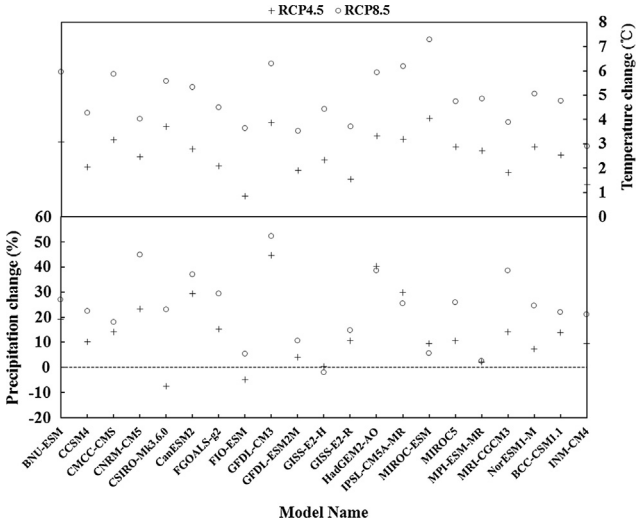

Fig. 10. Projected changes in mean annual temperature and precipitation by comparing the future period (2075–2100) against the historical period (1975–2000).

tion would be impacted by climate change based on ESM projections. For temperature, while the results of different ESMs diverged, all ESMs predicted a temperature increase for all months. On average, the most significant increase in temperature occurred during December or January. For precipitation, a divergence in projections was only evident for the wet season; mainly June through September. Some models predicted decreases in precipitation in certain months. On average, the most significant increase in precipitation occurred in July or August.

In the study area, groundwater typically accounted for 60–70% of the total water supply. The sensitivity analysis in Section 3.4 revealed that, with regard to overall quantity, the groundwater resource is more vulnerable in a changing climate than the surface water resource. Thus, sustainable utilization of groundwater under

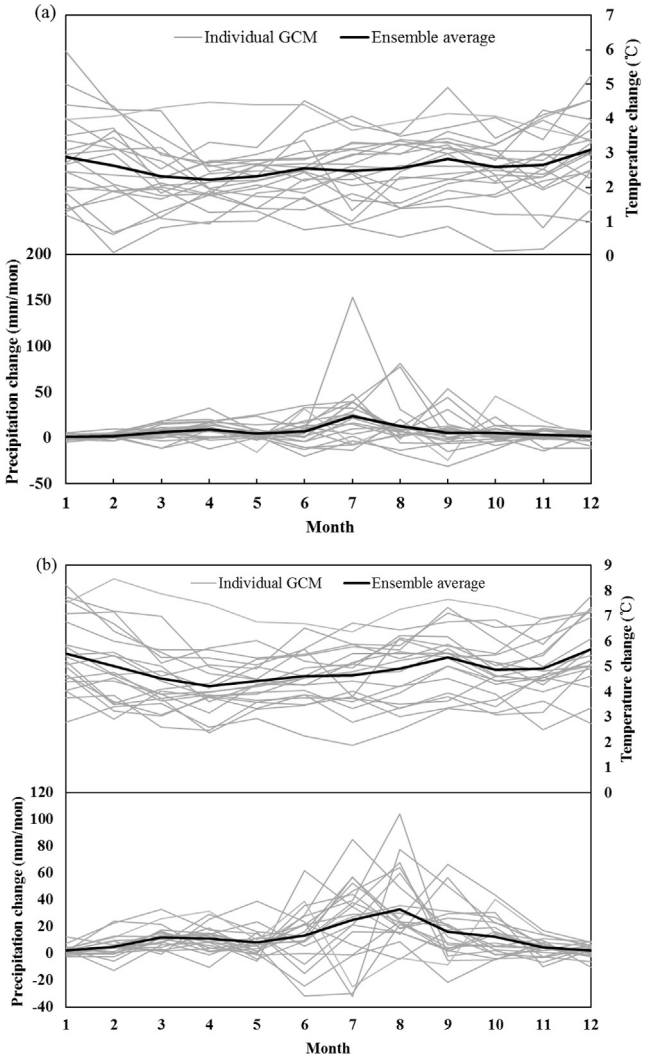

Fig. 11. Projected changes in average monthly temperature and precipitation by comparing the future period (2075–2100) against the historical period (1975–2000). (a) RCP4.5 and (b) RCP8.5.

climatic uncertainty represents a great challenge in this area. Fig. 12 shows the groundwater storage decline simulated by the GSFLOW model under the historical scenario and the two emission scenarios. By comparing the bars against the dashed line, it can be found that, under RCP4.5, 11 ESM projections led to an accelerated decline, where the largest acceleration was produced by CSIRO-Mk3.6.0. Similarly, under RCP8.5, 18 ESM projections resulted in an accelerated decline, where the largest acceleration was produced by MIROC-ESM. The number of ESMs with an accelerating effect is a good indicator of the groundwater depletion risk induced by climate change. Clearly, climate change under RCP4.5 would cause a moderate risk for groundwater depletion (11 out of 21 ESMs), but under the high emission scenario (RCP8.5), the risk would be substantial (18 out of 21 ESMs). Groundwater resources show vulnerability to future climate change and face the risk of accelerated decline in this area, which is consistent with the results from the former sensitivity analysis. The robustness of our methodology and conclusion was also verified.

It is evident that groundwater in the study area has been significantly over-pumped, and the storage decline is likely to be exacerbated by climate change. It represents a great challenge to water resource management, not only in the Luanhe Plain but also in the entire North China Plain. Thus, the interaction between groundwater management and climate change was further investigated. The GSFLOW model was re-run for the historical climate scenario (1975–2000) and 42 future climate scenarios (2075–2100) at three reduced levels of pumping—75%, 50% and 25% of the historical level. It was also assumed that the reduction in groundwater pumping equaled the reduction of irrigation. Note that, according to the GSFLOW model, even if pumping is reduced to 25% of the historical level, groundwater storage in this area would still decrease. Fig. 13a plots the numbers of ESMs with accelerated effects at the four pumping levels. Interestingly, under RCP4.5, the groundwater depletion risk indicated by the number of ESMs would not vary with the pumping level; however, under RCP8.5, the risk would increase rapidly with enhanced pumping. This implies that, if climate change is substantial, a reduction in groundwater pumping would not only alleviate the decline in groundwater storage (i.e., the direct effect) but would also mitigate the negative impact of climate change on storage (i.e., the indirect effect) by altering the water cycle. Fig. 13b further illustrates the additional storage decline caused by climate change under RCP8.5. It shows that, on average, the climate-induced storage decline would increase as pumping is enhanced; however, its uncertainty according to the 21 ESMs would also increase significantly. Overall, Fig. 13 suggests that regulation of groundwater pumping is imperative for water security in this area, especially when future climate change, as well as its huge uncertainty, is taken into consideration.

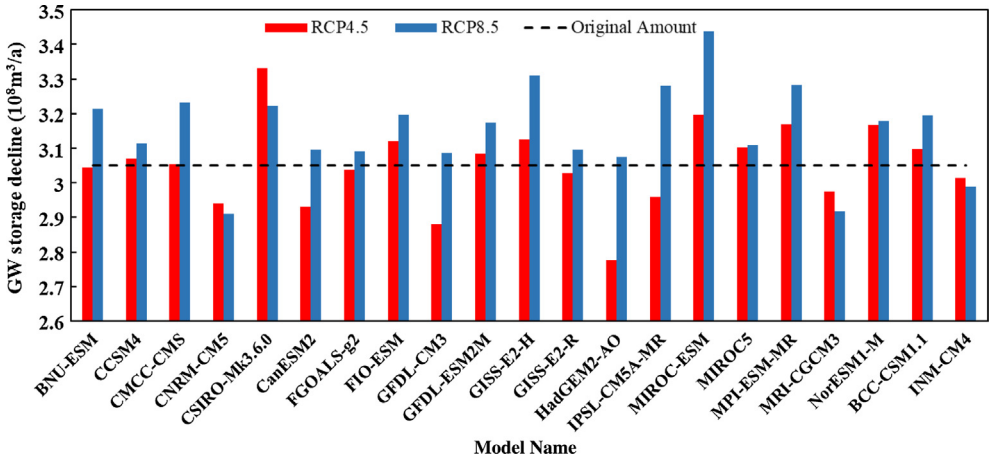

Fig. 12. Groundwater storage declines simulated by the GSFLOW model under different climate scenarios. The dashed line indicates the decline under the historical climate condition.

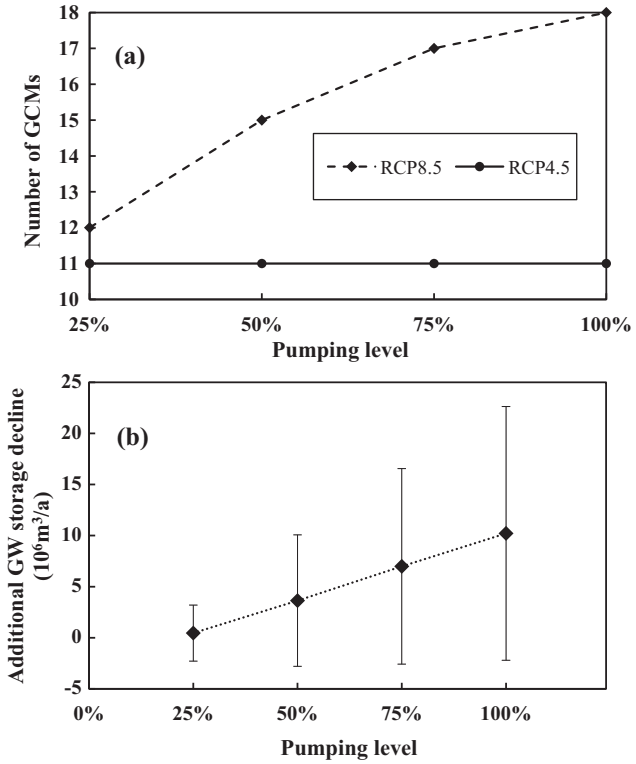

Fig. 13. Responses of the groundwater resource to future climate change under different levels of pumping. (a) Number of ESMs that would lead to an accelerated groundwater storage decline and (b) additional groundwater storage decline induced by climate change.

4. Conclusions

This study successfully developed an integrated SW-GW model for the Luanhe Plain, a typical coastal area in northern China, under significant data scarcity. It also developed an integrated modeling-based approach to attribute variation in water resources to climate variability and human activities. The sensitivity of the hydrological processes to climate change was analyzed, and the risks of groundwater depletion under climatic uncertainty were investigated using downscaled data from multiple ESMs.

The major study findings include the following. First, both the climate factor and human factor had a significant impact on the integrated SW-GW system, but they played different roles in different aspects of the system. For example, the human factor dominated variation in groundwater level (or storage), whereas the change in basin-wide ET was largely controlled by the climate factor. Second, complicated interactions existed between the climate factor and the human factor. Their impacts may either counteract each other or synergize with each other, depending on the concerned part of the hydrological cycle. For example, the interaction between these two factors intensified their individual impacts on ET. Third, in this representative coastal area of northern China, the groundwater resource was found to be much more vulnerable to projected climate change than surface water resources with regard to overall quantity. It is highly possible that future climate change will amplify the risk of groundwater depletion, and the climate-induced risk of depletion could be dependent on pumping intensity. In the Luanhe Plain, regulation of groundwater pumping appeared to be an imperative adaptation measure for water security under climatic uncertainty.

Overall, this study demonstrated that the complicated interaction between climate change and human activities is changing the water cycle in a typical coastal area. The applicability and value of an integrated modeling-based approach was well represented in the study results. Some important issues deserve further research. In this study, the agricultural water use was determined externally and assumed to be unchanged or reduced by pumping regulations under future climate conditions. Future studies may consider an integrated surface water-groundwater model with functionality of irrigation simulation (Condon and Maxwell, 2013), where potential changes in agricultural water use due to climate change can be directly investigated. In addition, a more sophisticated downscaling approach may be employed to further investigate the impact of climate change on extreme events.

Acknowledgments

This work was funded by the National Natural Science Foundation of China (No. 41622111; No. 91647201; No. 41501024) and the Shenzhen Municipal Science and Technology Innovation Committee (No. JCYJ20160530190411804). Additional support was provided by the Southern University of Science and Technology (No. G01296001).

References

Ajami, H., McCabe, M.F., Evans, J.P., Stisen, S., 2014. Assessing the impact of model spin-up on surface water-groundwater interactions using an integrated hydrologic model. Water. Resour. Res. 50 (3), 2636–2656. https://doi.org/10.1002/2013wr014258.

Ali, R. et al., 2012. Potential climate change impacts on groundwater resources of south-western Australia. J. Hydrol. 475, 456–472. https://doi.org/10.1016/j.jhydrol.2012.04.043.

Arnold, J.G., Moriasi, D.N., Gassman, P.W., Abbaspour, K.C., White, M.J., Srinivasan, R., Santhi, C., Harmel, R.D., Griensven, A. Van, VanLiew, M.W., Kannan, N., Jha, M. K., 2012. SWAT: model use, calibration, and validation. Trans. ASABE 55 (4), 1491–1508.

Bao, Z.X. et al., 2012. Attribution for decreasing streamflow of the Haihe River basin, northern China: climate variability or human activities? J. Hydrol. 460, 117–129. https://doi.org/10.1016/j.jhydrol.2012.06.054.

Benini, L., Antonellini, M., Laghi, M., Mollema, P.N., 2016. Assessment of water resources availability and groundwater salinization in future climate and land use change scenarios: a case study from a Coastal Drainage Basin in Italy. Water. Resour. Manag. 30 (2), 731–745. https://doi.org/10.1007/s11269-015-1187-4.

Brinson, M. et al., 2013. A rapid watershed assessment approach for assessing the condition of small, coastal watersheds: Protocol and case study. Ocean. Coast. Manage. 71, 238–255. https://doi.org/10.1016/j.ocecoaman.2012.08.006.

Brunner, P., Simmons, C.T., 2012. HydroGeoSphere: a fully integrated. Phys. Based Hydrol. Model. Ground Water 50 (2), 170–176. https://doi.org/10.1111/j.1745-6584.2011.00882.x.

Camporese, M., Paniconi, C., Putti, M., Orlandini, S., 2010. Surface-subsurface flow modeling with path-based runoff routing, boundary condition-based coupling, and assimilation of multisource observation data. Water. Resour. Res. 46, 22. https://doi.org/10.1029/2008wr007536.

Cao, G.L., Zheng, C.M., Scanlon, B.R., Liu, J., Li, W.P., 2013. Use of flow modeling to assess sustainability of groundwater resources in the North China Plain. Water. Resour. Res. 49 (1), 159–175. https://doi.org/10.1029/2012wr011899.

Carroll, R.W.H. et al., 2017. Evaluating mountain meadow groundwater response to Pinyon-Juniper and temperature in a great basin watershed. Ecohydrology 10 (1), 18. https://doi.org/10.1002/eco.1792.

Chen, C., Greene, A.M., Robertson, A.W., Baethgen, W.E., Eamus, D., 2013. Scenario development for estimating potential climate change impacts on crop production in the North China Plain. Int. J. Climatol. 33 (15), 3124–3140. https://doi.org/10.1002/joc.3648.

Chen, D., Hu, M., Guo, Y., Dahlgren, R.A., 2016. Changes in river water temperature between 1980 and 2012 in Yongan watershed, eastern China: Magnitude, drivers and models. J. Hydrol. 533, 191–199. https://doi.org/10.1016/j.jhydrol.2015.12.005.

Chen, J., Brissette, F.P., Leconte, R., 2011. Uncertainty of downscaling method in quantifying the impact of climate change on hydrology. J. Hydrol. 401 (3–4), 190–202. https://doi.org/10.1016/j.jhydrol.2011.02.020.

Chen, J.X. et al., 2014. The mechanism and scenarios of how mean annual runoff varies with climate change in Asian monsoon areas. J. Hydrol. 517, 595–606. https://doi.org/10.1016/j.jhydrol.2014.05.075.

Condon, L.E., Maxwell, R.M., 2013. Implementation of a linear optimization water allocation algorithm into a fully integrated physical hydrology model. Adv. Water. Resour 60, 135–147. https://doi.org/10.1016/j.advwatres.2013.07.012.

Diaz-Nieto, J., Wilby, R.L., 2005. A comparison of statistical downscaling and climate change factor methods: impacts on low flows in the River Thames, United Kingdom. Clim. Change 69 (2), 245–268. https://doi.org/10.1007/s10584-005-1157-6.

Doherty, J., Hunt, R.J., 2009. Two statistics for evaluating parameter identifiability and error reduction. J. Hydrol. 366 (1–4), 119–127. https://doi.org/10.1016/j.jhydrol.2008.12.018.

Du, H., Xia, J., Zeng, S.D., She, D.X., Liu, J.J., 2014. Variations and statistical probability characteristic analysis of extreme precipitation events under climate change in Haihe River Basin. China. Hydrol. Process. 28 (3), 913–925. https://doi.org/10.1002/hyp.9606.

Fu, G., Charles, S.P., Yu, j., 2009. Decadal climatic variability, trends, and future scenarios for the north China plain. J. Clim. 22 (8), 2111–2123. https://doi.org/10.1175/2008jcli2605.1.

Goderniaux, P. et al., 2009. Large scale surface-subsurface hydrological model to assess climate change impacts on groundwater reserves. J. Hydrol. 373 (1–2), 122–138. https://doi.org/10.1016/j.jhydrol.2009.04.017.

Gorelick, S.M., Zheng, C., 2015. Global change and the groundwater management challenge. Water. Resour. Res. 51 (5), 3031–3051. https://doi.org/10.1002/2014wr016825.

Graham, D.N., Butts, M.B., 2005. Flexible, integrated watershed modelling with MIKE SHE. In: V.P., S., D.K., F (Eds), Watershed Models. CRC Press, pp. 245–272.

Green, T.R. et al., 2011. Beneath the surface of global change: Impacts of climate change on groundwater. J. Hydrol. 405 (3–4), 532–560. https://doi.org/10.1016/j.jhydrol.2011.05.002.

Haihe River Chronicle Compilation Committee, Haihe River Water Resources Commission, China, 1994. Luanhe River Chronicle (in Chinese). Hebei People Press, Shijiazhuang.

Hamed, K.H., Rao, A.R., 1998. A modified Mann-Kendall trend test for autocorrelated data. J. Hydrol. 204 (1–4), 182–196. https://doi.org/10.1016/s0022-1694(97)00125-x.

Harbaug, A.W., 2005. MODFLOW-2005. The U.S. Geological Survey modular groundwater model-the ground-water flow process. USGS Techniques and Methods: 6-A16. Available at: http://pubs.usgs.gov/tm/2005/tm6A16/PDF.htm (accessed on 12/08/2017).

Hassan, S.M.T., Lubczynski, M.W., Niswonger, R.G., Su, Z., 2014. Surface-groundwater interactions in hard rocks in Sardon Catchment of western Spain: An integrated modeling approach. J. Hydrol. 517, 390–410. https://doi.org/10.1016/j.jhydrol.2014.05.026.

Hirsch, R.M., Slack, J.R., Smith, R.A., 1982. Techniques of trend analysis for monthly water quality data. Water. Resour. Res. 18 (1), 107–121. https://doi.org/10.1029/WR018i001p00107.

Huang, J., Zhang, Z., Feng, Y., Hong, H., 2013. Hydrologic response to climate change and human activities in a subtropical coastal watershed of southeast China. Reg. Environ. Change. 13 (6), 1195–1210. https://doi.org/10.1007/s10113-013-0432-8.

Huang, R., Lin, Y., 1991. Industrial development in the eastern Hebei province and water resources exploitation of the Luanhe river (in Chinese). J. Nat. Resour. 6 (4), 361–369.

Huntington, J.L., Niswonger, R.G., 2012. Role of surface-water and groundwater interactions on projected summertime streamflow in snow dominated regions: An integrated modeling approach. Water. Resour. Res. 48 (11), W11524. https://doi.org/10.1029/2012WR012319.

Jackson, C.R., Meister, R., Prudhomme, C., 2011. Modelling the effects of climate change and its uncertainty on UK Chalk groundwater resources from an ensemble of global climate model projections. J. Hydrol. 399 (1–2), 12–28. https://doi.org/10.1016/j.jhydrol.2010.12.028.

Jiang, Y., Liu, C.M., Li, X.Y., 2015. Hydrological Impacts of Climate Change Simulated by HIMS Models in the Luanhe River Basin, North China. Water. Resour. Manag. 29 (4), 1365–1384. https://doi.org/10.1007/s11269-014-0881-y.

Jiang, Y., Liu, C., Li, X., Liu, L., Wang, H., 2015. Rainfall-runoff modeling, parameter estimation and sensitivity analysis in a semiarid catchment. Environ. Model. Softw. 67, 72–88. https://doi.org/10.1016/j.envsoft.2015.01.008.

Klove, B. et al., 2014. Climate change impacts on groundwater and dependent ecosystems. J. Hydrol. 518, 250–266. https://doi.org/10.1016/j.jhydrol.2013.06.037.

Krause, S., Jacobs, J., Bronstert, A., 2007. Modelling the impacts of land-use and drainage density on the water balance of a lowland-floodplain landscape in northeast Germany. Ecol. Model. 200 (3–4), 475–492. https://doi.org/10.1016/j.ecolmodel.2006.08.015.

Lørup, J.K., Refsgaard, J.C., Mazvimavi, D., 1998. Assessing the effect of land use change on catchment runoff by combined use of statistical tests and hydrological modelling: Case studies from Zimbabwe. J. Hydrol. 205 (3), 147–163. https://doi.org/10.1016/S0168-1176(97)00311-9.

Landes, A.A.L. et al., 2014. Investigating the respective impacts of groundwater exploitation and climate change on wetland extension over 150 years. J. Hydrol. 509, 367–378. https://doi.org/10.1016/j.jhydrol.2013.11.039.

Leavesley, G.H., Lichty, R.W., Troutman, B.M., Saindon, L.G., 1983. Precipitation-runoff modeling system: User's manual. USGS Water-Resources Investigations Report: 83-4238, 206pp. Available at: http://pubs.usgs.gov/wri/1983/4238/report.pdf (accessed on 12/08/2017).

Li, L.C. et al., 2015. Implications of modelled climate and land cover changes on runoff in the Middle Route of the South to North Water Transfer Project in China. Water. Resour. Manag. 29 (8), 2563–2579. https://doi.org/10.1007/s11269-015-0957-3.

Li, Q., Li, P., Li, H., Yu, M., 2014a. Drought assessment using a multivariate drought index in the Luanhe River basin of Northern China. Stoch. Env. Res. Risk. A. 29 (6), 1509–1520. https://doi.org/10.1007/s00477-014-0982-4.

Li, X., Li, G.M., Zhang, Y., 2014b. Identifying major factors affecting groundwater change in the North China Plain with grey relational analysis. Water 6 (6), 1581–1600. https://doi.org/10.3390/w6061581.

Li, Z., Liu, W.-Z., Zhang, X.-C., Zheng, F.-L., 2009. Impacts of land use change and climate variability on hydrology in an agricultural catchment on the Loess Plateau of China. J. Hydrol. 377 (1–2), 35–42. https://doi.org/10.1016/j.jhydrol.2009.08.007.

Liu, C.M., Yu, J.J., Kendy, E., 2001. Groundwater exploitation and its impact on the environment in the North China Plain. Water Int. 26 (2), 265–272.

Liu, J., Cao, G., Zheng, C., 2011. Sustainability of groundwater resources in the North China Plain. In: Sustaining Groundwater Resources, J. A. A. Jones (Ed). Sustaining Groundwater Resources. International Year of Planet Earth. doi:10.1007/978-90-481-3426-7_5. Springer, New York.

Liu, J., Zheng, C.M., Zheng, L., Lei, Y.P., 2008. Ground water sustainability: methodology and application to the North China Plain. Ground Water 46 (6), 897–909. https://doi.org/10.1111/j.1745-6584.2008.00486.x.

Markstrom, S.L., Niswonger, R.G., Regan, R.S., Prudic, D.E., Barlow, P.M., 2008. GSFLOW-Coupled Ground-water and Surface-water FLOW Model Based on the Integration of the Precipitation-runoff Modeling System (PRMS) and the Modular Ground-water Flow Model (MODFLOW-2005). U.S. Geological Survey Techniques and Methods 6-D1, 240pp. Available at: http://pubs.usgs.gov/tm/tm6d1/pdf/tm6d1.pdf (accessed on 12/08/2017).

Miller, N.L., Bashford, K.E., Strem, E., 2003. Potential impacts of climate change on California hydrology. J. Am. Water. Resour. As. 39 (4), 771–784. https://doi.org/10.1111/j.1752-1688.2003.tb04404.x.

Morrison, J., Quick, M.C., Foreman, M.G.G., 2002. Climate change in the Fraser River watershed: flow and temperature projections. J. Hydrol. 263 (1–4), 230–244. https://doi.org/10.1016/s0022-1694(02)00065-3.

Ouyang, F. et al., 2015. Impacts of climate change under CMIP5 RCP scenarios on streamflow in the Huangnizhuang catchment. Stoch. Env. Res. Risk. A 29 (7), 1781–1795. https://doi.org/10.1007/s00477-014-1018-9.

Ouyang, W., Shi, Y., Hao, F., Jiao, W., 2016. A comparison of general circulation models and their application to temperature change assessments in a high-latitude agricultural area in northeastern China. Clim. Dyn. 47 (1), 651–666. https://doi.org/10.1007/s00382-015-2861-1.

Pérez, A.J., Abrahão, R., Causapé, J., Cirpka, O.A., Bürger, C.M., 2011. Simulating the transition of a semi-arid rainfed catchment towards irrigation agriculture. J. Hydrol. 409 (3–4), 663–681. https://doi.org/10.1016/j.jhydrol.2011.08.061.

Pokhrel, Y.N. et al., 2015. Incorporation of groundwater pumping in a global Land Surface Model with the representation of human impacts. Water. Resour. Res. 51 (1), 78–96. https://doi.org/10.1002/2014wr015602.

Pulido-Velazquez, M. et al., 2015. Integrated assessment of the impact of climate and land use changes on groundwater quantity and quality in the Mancha Oriental system (Spain). Hydrol. Earth. Syst. Sci. 19 (4), 1677–1693. https://doi.org/10.5194/hess-19-1677-2015.

Schnorbus, M., Werner, A., Bennett, K., 2014. Impacts of climate change in three hydrologic regimes in British Columbia. Canada. Hydrol. Process. 28 (3), 1170–1189. https://doi.org/10.1002/hyp.9661.

Sen, P.K., 1968. Estimates of the regression coefficient based on Kendall's Tau. J. Am. Stat. Assoc. 63 (324), 1379–1389. https://doi.org/10.1080/01621459.1968.10480934.

Shen, C., Phanikumar, M.S., 2010. A process-based, distributed hydrologic model based on a large-scale method for surface–subsurface coupling. Adv. Water. Resour 33 (12), 1524–1541. https://doi.org/10.1016/j.advwatres.2010.09.002.

Sreeja, K.G., Madhusoodhanan, C.G., Eldho, T.I., 2016. Coastal zones in integrated river basin management in the West Coast of India: Delineation, boundary issues and implications. Ocean. Coast. Manage. 119, 1–13. https://doi.org/10.1016/j.ocecoaman.2015.09.017.

Stefanova, A., Krysanova, V., Hesse, C., Lillebo, A.I., 2015. Climate change impact assessment on water inflow to a coastal lagoon: the Ria de Aveiro watershed, Portugal. Hydrolog. Sci. J. 60 (5), 929–948. https://doi.org/10.1080/02626667.2014.983518.

Surfleet, C.G., Tullos, D., 2013. Uncertainty in hydrologic modelling for estimating hydrologic response due to climate change (Santiam River, Oregon). Hydrol. Process. 27 (25), 3560–3576. https://doi.org/10.1002/hyp.9485.

Teatini, P., Ferronato, M., Gambolati, G., Gonella, M., 2006. Groundwater pumping and land subsidence in the Emilia-Romagna coastland, Italy: modeling the past occurrence and the future trend. Water. Resour. Res., 42(1). doi:10.1029/2005wr004242.

Theil, H., 1950. A rank-invariant method of linear and polynomial regression analysis, part 3. Proceedings of Koninalijke Nederlandse Akademie van Weinenschatpen A 53, 1397–1412.

Therrien, R., McLaren, R.G., Sudicky, E.A., Panday, S.M., 2010. HydroGeoSphere A Three-dimensional Numerical Model Describing Fully-integrated Subsurface and Surface Flow and Solute Transport. Technical report.

Tian, Y. et al., 2015. Modeling surface water-groundwater interaction in arid and semi-arid regions with intensive agriculture. Environ. Model. Softw. 63, 170–184. https://doi.org/10.1016/j.envsoft.2014.10.011.

van Vuuren, D.P. et al., 2011. The representative concentration pathways: an overview. Clim. Change 109 (1–2), 5–31. https://doi.org/10.1007/s10584-011-0148-z.

VanderKwaak, J.E., Loague, K., 2001. Hydrologic-Response simulations for the R-5 catchment with a comprehensive physics-based model. Water. Resour. Res. 37 (4), 999–1013. https://doi.org/10.1029/2000WR900272.

Wada, Y. et al., 2010. Global depletion of groundwater resources. Geophys. Res. Lett. 37, 5. https://doi.org/10.1029/2010gl044571.
Wang, Q., Liu, J., 2010. Analyzing the impact of climate change and human activity on the water resources change in the lower reach of Luan River (in Chinese). China Water Resour. (15):41–44.
Wang, S., Huang, R., Ding, Y., 2002. Improvements of a distributed hydrology model DHSVM and its climatological- hydrological off-line simulation experiments (in Chinese). Acta. Meteorol. Sin. 60 (3), 290–300.
Wang, W. et al., 2013. Quantitative assessment of the impact of climate variability and human activities on runoff changes: a case study in four catchments of the Haihe River basin, China. Hydrol. Process. 27 (8), 1158–1174. https://doi.org/10.1002/hyp.9299.
Wang, W.G. et al., 2015. Spatial and temporal variations in hydro-climatic variables and runoff in response to climate change in the Luanhe River basin. China. Stoch. Env. Res. Risk. A 29 (4), 1117–1133. https://doi.org/10.1007/s00477-014-1003-3.
Werner, A.D. et al., 2013. Seawater intrusion processes, investigation and management: recent advances and future challenges. Adv. Water. Resour. 51, 3–26. https://doi.org/10.1016/j.advwatres.2012.03.004.
White, M.D., Greer, K.A., 2006. The effects of watershed urbanization on the stream hydrology and riparian vegetation of Los Penasquitos Creek, California. Landscape Urban Plan. 74 (2), 125–138. https://doi.org/10.1016/j.landurbplan.2004.11.015.
Wilby, R.L., Harris, I., 2006. A framework for assessing uncertainties in climate change impacts: Low-flow scenarios for the River Thames, UK. Water. Resour. Res. 42 (2), 10. https://doi.org/10.1029/2005wr004065.
Wu, B. et al., 2014. Systematic assessment of the uncertainty in integrated surface water-groundwater modeling based on the probabilistic collocation method. Water. Resour. Res. 50 (7), 5848–5865. https://doi.org/10.1002/2014wr015366.
Wu, Y., Chen, J., 2013. Analyzing the water budget and hydrological characteristics and responses to land use in a monsoonal climate river basin in South China. Environ. Manage. 51 (6), 1174–1186. https://doi.org/10.1007/s00267-013-0045-5.
Xia, Z., Li, Q., 2001. Study on soil water resource and its evaluating methodology (in Chinese). Adv. Water Sci. 12 (4), 535–540.
Xing, W.Q. et al., 2014. Changes of reference evapotranspiration in the Haihe River Basin: Present observations and future projection from climatic variables through multi-model ensemble. Glob. Planet. Change 115, 1–15. https://doi.org/10.1016/j.gloplacha.2014.01.004.
Yan, D.H., Wang, G., Wang, H., Qin, T.L., 2012. Assessing ecological land use and water demand of river systems: a case study in Luanhe River, North China. Hydrol. Earth. Syst. Sc. 16 (8), 2469–2483. https://doi.org/10.5194/hess-16-2469-2012.
Yao, Y., Zheng, C., Andrews, C., Zheng, Y., Zhang, A., Liu, J., 2017. What controls the partitioning between baseflow and mountain block recharge in the Qinghai-Tibet Plateau? Geophys. Res. Lett. 44 (16), 8352–8358. https://doi.org/10.1002/2017GL074344.
Yuan, F., Xie, Z.H., Liu, Q., Xia, J., 2005. Simulating hydrologic changes with climate change scenarios in the Haihe River Basin. Pedosphere 15 (5), 595–600.
Yue, S., Pilon, P., Phinney, B., Cavadias, G., 2002. The influence of autocorrelation on the ability to detect trend in hydrological series. Hydrol. Process. 16 (9), 1807–1829. https://doi.org/10.1002/hyp.1095.
Zhang, Z., Huang, J., Huang, Y., Hong, H., 2015. Streamflow variability response to climate change and cascade dams development in a coastal China watershed. Estuar. Coast. Shelf. S. 166, 209–217. https://doi.org/10.1016/j.ecss.2015.10.002.
Zhao, A., Zhu, X., Liu, X., Pan, Y., Zuo, D., 2016. Impacts of land use change and climate variability on green and blue water resources in the Weihe River Basin of northwest China. CATENA 137, 318–327. https://doi.org/10.1016/j.catena.2015.09.018.
Zhao, F.F., Zhang, L., Xu, Z.X., Scott, D.F., 2010. Evaluation of methods for estimating the effects of vegetation change and climate variability on streamflow. Water. Resour. Res. 46, 14. https://doi.org/10.1029/2009wr007702.
Zhao, H., 2009. The problems and countermeasures of the exploitation of groundwater in coastal plain of Luanhe River basin and east Hebei Province (in Chinese). Water Resourc. Protect. 25 (1), 27–33.